The BRAHMS Experiment at the Relativistic Heavy Ion Collider

Y. K. Lee for the BRAHMS Collaboration,[1,*] I. G. Bearden,[2] D. Beavis,[3] C. Besliu,[4] Y. Blyakhman,[5]
J. Brzychczyk,[6] B. Budick,[5] H. Bøggild,[2] C. Chasman,[3] C. H. Christensen,[2] P. Christiansen,[2]
J. Cibor,[7] R. Debbe,[3] E. Enger,[8] J. J. Gaardhøje,[2] K. Grotowski,[6] K. Hagel,[9] O. Hansen,[2]
A. Holm,[2] A. K. Holme,[8] H. Ito,[10] E. Jakobsen,[2] A. Jipa,[4] J. I. Jørdre,[11] F. Jundt,[12]
C. E. Jørgensen,[2] T. Keutgen,[9] E. J. Kim,[3] T. Kozik,[6] T. M. Larsen,[8] J. H. Lee,[3] Y. K. Lee,[1]
G. Løvhøiden,[8] Z. Majka,[6] A. Makeev,[9] B. McBreen,[3] M. Mikelsen,[8] M. Murray,[9] J. Natowitz,[9]
B. S. Nielsen,[2] J. Norris,[10] K. Olchanski,[3] J. Olness,[3] D. Ouerdane,[2] R. Płaneta,[6] F. Rami,[12]
D. Röhrich,[11] B. H. Samset,[8] D. Sandberg,[2] S. J. Sanders,[10] R. A. Sheetz,[3] Z. Sosin,[6] P. Staszel,[2]
T. F. Thorsteinsen,[11,†] T. S. Tveter,[8] F. Videbæk,[3] R. Wada,[9] A. Wieloch[6] and I. S. Zgura[4]

(BRAHMS Collaboration)

[1]*Johns Hopkins University, Baltimore, Maryland 21218, U.S.A.*
[2]*Niels Bohr Institute, University of Copenhagen, Denmark*
[3]*Brookhaven National Laboratory, Upton, New York 11973, U.S.A.*
[4]*University of Bucharest, Romania*
[5]*New York University, New York, New York 10003, U.S.A.*
[6]*Jagiellonian University, Krakow, Poland*
[7]*Institute of Nuclear Physics, Krakow, Poland*
[8]*University of Oslo, Department of Physics, Oslo, Norway*
[9]*Texas A&M University, College Station, Texas 77843, U.S.A.*
[10]*University of Kansas, Lawrence, Kansas 66049, U.S.A.*
[11]*University of Bergen, Department of Physics, Bergen, Norway*
[12]*Institut de Recherches Subatomiques and Université Louis Pasteur,Strasbourg, France*

The BRAHMS probes the hot and dense nuclear matter at the RHIC which has reached its design energy of $\sqrt{s_{NN}} = 200$ GeV for Au + Au collisions. The BRAHMS uses magnetic spectrometers for hadrons covering a large phase space $0 < y < 4$ with good particle identification and momentum resolution. A comprehensive investigation of multiplicity distributions of emitted charged particles is carried out. Ratios of yields of antiparticles to particles are also measured as a function of rapidity. Rapidity dependent net-proton yield indicates that substantial transparency has been achieved in these collisions. Transverse momentum spectra of charged hadrons are measured up to 5 GeV/c which indicates a significant medium effect when compared to nucleon + nucleon reference spectra.

PACS numbers: 25.75.Dw
Keywords: Relativistic heavy ion collider, BRAHAMS, Hot and dense nuclear matter, Multiplicity distribution, Rapidity distribution

I. INTRODUCTION

On this occasion of the fiftieth jubilee of the founding of the Korean Physical Society and the thirtieth jubilee of the birth of its Nuclear Physics Division it is befitting to discuss the new physics which the BRAHMS experiment is undertaking at the Relativistic Heavy Ion Collider (RHIC). In this presentation we would focus on the results of pseudorapidity density measurements of charged hadrons and the antiparticle-to-particle ratio measurements for Au + Au collisions at $\sqrt{s_{NN}} = 200$ GeV. The pseudorapidity densities $dN/d\eta$ are sensitive to the relative contributions of "soft" and "hard" scattering between partons [1, 2]. Detailed theoretical model based on gluon saturation [3] and also models based on perturbative QCD [1,4–6] exist for pseudorapidity densities which describe well the results of measurement at $\sqrt{s_{NN}} = 130$ GeV. The antiparticle-to-particle ratios are used in statistical model to test the level of equilibration and to determine the temperature and chemical potentials of hadrons at hadronization stage. We would briefly mention the results of preliminary analysis on the rapidity densities of hadrons over a wide range $|y| < 4$ and the high transverse momentum spectra as a function of rapidity and centrality.

*E-mail: yklee@jhu.edu
†Deceased

II. THE BRAHMS DETECTORS

The RHIC had two successful years of operation reaching the maximum design energy of $\sqrt{s_{NN}} = 200$ GeV for Au + Au collisions in 2001, and achieving a moderately successful polarized p-p collision in 2002. The primary goal of RHIC is to study the dense and hot nuclear matter, recreating environment similar to the early stage of the universe. Currently d + Au beams are in development at RHIC. The RHIC has two large detectors, PHENIX and STAR, and two small detectors, PHOBOS and BRAHMS.

The BRAHMS is a combination of two independent movable magnetic spectrometers: the midrapidity spectrometer and the forward spectrometer, exploring large phase space with good particle identification [7,8]. The midrapidity spectrometer (MRS) of the BRAHMS consists of two TPC's, one magnet and a time-of-flight wall. It can be positioned over angular range from $35°$ to $95°$. It has rapidity coverage of $-0.1 < y < 3.4$ for pions and $-0.1 < y < 4$ for protons. A new threshold Cerenkov detector is being readied to extend the particle identification range of MRS. The forward spectrometer (FS) divides into the front and the back spectrometers which can be positioned separately. The combined forward spectrometer can be positioned over an angular range from $2.3°$ to $30°$. The combined FS includes four magnets, two TPC's, drift chambers, two time-of-flight hodoscopes and two Cerenkov counters. The ring-imaging Cerenkov counter gives πK separation to 25 GeV and KP separation to 35 GeV.

The BRAHMS spectrometers have four global detectors for determining the location of the collision vertex, the time of the collision, the collision centrality and the charged particle densities [8]. The zero degree calorimeters measure the spectator neutrons from the collisions. The beam-beam counters (BB) consist of two sets of arrays of Cerenkov counters at 2.20 m from the intersection region and provide the start-time signals for the trigger system and also provide the point of intersection with an accuracy of 0.9 cm.

The multiplicity arrays (MA) which function to measure the centrality of the collisions consist of the silicon multiplicity array (SiMA) of modestly segmented silicon strip detectors and the scintillator tile multiplicity arrays (TMA) which form concentric cylindrical barrels about the beam pipe near the intersection regions.

III. PSEUDORAPIDITY DISTRIBUTION OF CHARGED PARTICLES

For the collisions of Au + Au at $\sqrt{s_{NN}} = 200$ GeV we measured the pseudorapidity distributions of charged particles in the range $-4.7 \leq \eta \leq 4.7$ as a function of collision centrality. The results show that production of charged particles at midrapidity increases by
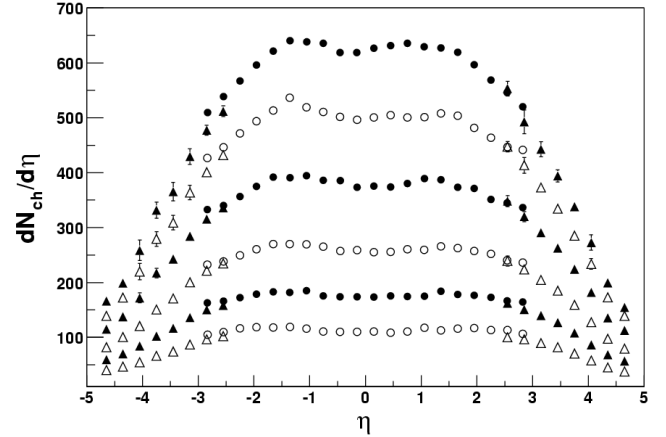

Fig. 1. Distributions of $dN_{\mathrm{ch}}/d\eta$ for centrality ranges of, top to bottom, 0–5 %, 5–10 %, 10–20 %, 20–30 %, 30–40 % and 40–50 %. The SiMA and BB results are indicated by the circles and triangles, respectively.

14 ± 1 % for the most central collisions relative to $\sqrt{s_{NN}} = 130$ GeV collisions [7,10–12], in agreement with the results of the PHOBOS experiment [13].

Particle densities are deduced from the observed energy loss in the SiMA elements using GEANT simulations [14] to relate energy loss to the number of particles hitting a given detector element [7]. The BB arrays of two sets of Cherenkov counters are used to measure in the pseudorapidity range $2.1 \leq |\eta| \leq 4.7$. Reaction centrality is determined by selecting different regions in the total multiplicity distribution in either the MA or BB counter arrays. In general, statistical errors on the measurements are less than 1 %, while the estimated systematic errors are 8 % and 10 % for the SiMA and BB arrays, respectively. For more details of the methods used here see [7] which is the reference to our measurements at $\sqrt{s_{NN}} = 130$ GeV.

Figure 1 shows the measured pseudorapidity distributions for charged particles for several centrality cuts. For the most central collisions (0–5 %) the charged particle density reaches $dN_{\mathrm{ch}}/d\eta = 625 \pm 55$ at midrapidity. This corresponds to 3.5 ± 0.3 charged particles per participating baryon pair.

In order to see if the data support the limiting fragmentation picture which predicts that the excitations of the fragment baryons saturate at a moderate collision energy, independently of system size [7, 15], data are plotted as a function of pseudorapidity and shifted by the beam energy. Figure 2 shows that the charged particle multiplicities in an interval of approximately 0.5–1.5 units below the beam rapidity are independent of the collision centrality and energy, from CERN-SPS energy ($\sqrt{s_{NN}} = 17$ GeV) [16] to the present RHIC energy in confirmation of the limiting fragmentation picture.

Several successful theoretical models are proposed to interpret the pseudorapidity density at $\sqrt{s_{NN}} = 130$ GeV with formalism for extrapolation to $\sqrt{s_{NN}} = 200$ GeV
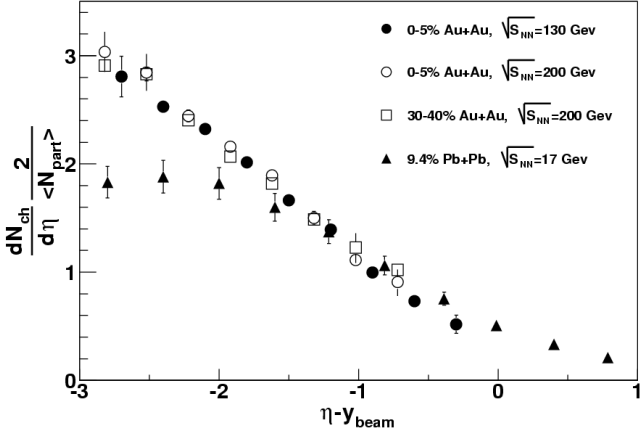
Fig. 2. Charged particle densities normalized to the number of participant pairs for the present 0–5 % central (open circles) and 30–40 % central (open squares) Au + Au results at $\sqrt{s_{NN}} = 200$ GeV, the BRAHMS Au + Au results [7] at $\sqrt{s_{NN}} = 130$ GeV (closed circles) and the 9.4 % central Pb+Pb data at $\sqrt{s_{NN}} = 17$ GeV (closed triangles) of Ref. 16. Data at different beam energies are plotted as a function of the pseudorapidity shifted by the relevant beam rapidity. Representative total uncertainties are shown for a few Au + Au points.

Fig. 3. (a-d) Measured $dN_{\rm ch}/d\eta$ distributions for centrality ranges of 0–5 %, 10–20 %, 20–30 % and 40–50 %. Theoretical predictions by Kharzeev and Levin (solid line) and by the AMPT model (dashed line) are also shown. Result from $p\bar{p}$ collisions at this energy [17], scaled by the Au + Au values of $N_{\rm part}/2$, are shown with stars (a,d).

data. We will compare our results with the predictions of two models. The parton saturation model of Kharzeev and Levin [3] assumes large number of gluons in the early stage of collisions. The model provides simple analytical scaling function which embodies the predictions of high density QCD on the energy, centrality, rapidity and atomic number dependence of hadron multiplicity. The AMPT model [4–6] is a cascade model based on the HIJING model [1] inspired by perturbative QCD and multiple minijets. The AMPT model builds on the HIJING model by including the final-state rescattering of produced particles. Figure 3 presents the $dN_{\rm ch}/d\eta$ distributions obtained averaging the negative and positive halves of the measured distributions to further decrease errors. The solid lines are calculations using the model of Kharzeev and Levin and the dashed lines are the results of calculations with the AMPT model. The similar distributions [17] from $p\bar{p}$ collisions at $\sqrt{s} = 200$ GeV, scaled by the corresponding number of Au + Au participant pairs, are also shown. The gluon saturation model of Kharzeev and Levin is quite successful in reproducing the current data, but the AMPT model based on different perspective can also reproduce the data quite well.

IV. CHARGED ANTIPARTICLE-TO-PARTICLE RATIOS

The ratios have been measured with the MRS and FS set at various angles. The details of the methods of measurements are given in the previous publi-
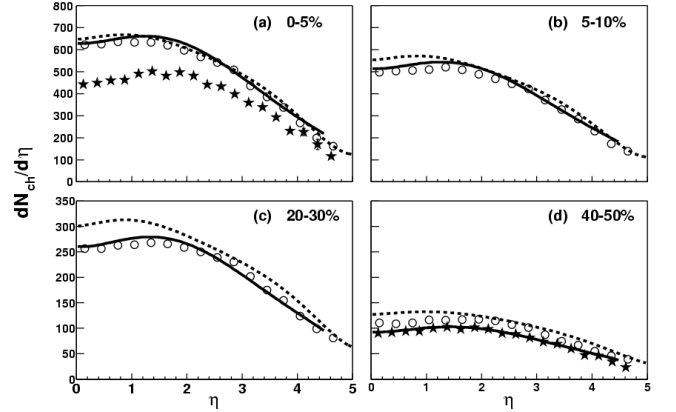
cation [18] which describes the ratios measurements at $\sqrt{s_{NN}} = 130$ GeV and in Ref. 19.

At midrapidity, the measured antiparticle to particle ratios are 0.75 ± 0.04 ($\bar{p}/p$), 0.95 ± 0.05 (K^-/K^+) and 1.01 ± 0.04 (π^-/π^+). Recent PHOBOS measurements [20] are consistent with the $y = 0$ measurements presented here. At higher rapidity the ratio for pions is consistent with 1 but other ratios are $K^-/K^+ = 0.67 \pm 0.06$ at $y = 3.05$ and $\bar{p}/p = 0.23 \pm 0.03$ at $y = 3.1$. The ratios have been corrected for absorption and production of secondary particles in the material traversed. Corrections are applied for the losses of antiprotons due to annihilations and background interactions. The effect of K decay losses cancel out in taking the ratios.

Figure 4 shows the π^-/π^+, K^-/K^+ and $\bar{p}/p$ ratios as a function of rapidity. Statistical errors are shown as vertical error bars, while systematic plus statistical errors are indicated by the caps. Systematic uncertainties are estimated as 4 % primarily from the normalizations between opposite polarity settings. The $\bar{p}/p$ ratio 0.75 ± 0.04 at $y = 0$ exceeds the ratio measured in Au + Au collisions at $\sqrt{s_{NN}} = 130$ GeV [18,21,22] by about 17 %.

The statistical model of Braun-Munzinger *et al.* [23] with two parameters, T for temperature and μ_B for baryon chemical potential, derives the energy dependence of particle ratios with parameter inputs from data for $\sqrt{s_{NN}} = 130$ GeV. On this basis the model leads to a prediction for $\sqrt{s_{NN}} = 200$ GeV of $T = 177 \pm 7$ MeV, $\mu_B = 29 \pm 8$ MeV and thus $\bar{p}/p = 0.752$, $K^-/K^+ = 0.932$ and $\pi^-/\pi^+ = 1.004$. The agreement with our current result is quite good.

A comparison of the K^-/K^+ and $\bar{p}/p$ ratios shows interesting correlations giving another opportunity to test the statistical model. Such correlation is shown in Fig. 5. Also shown are similar ratios determined at AGS [24] and SPS energies [25,26]. The dotted line in Fig. 5 showing
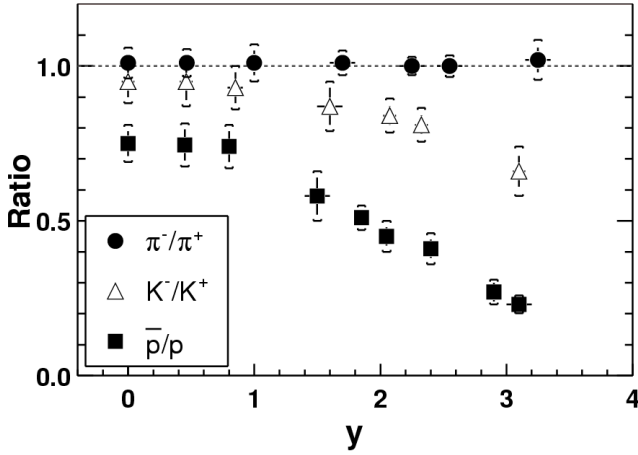
Fig. 4. Antiparticle-to-particle ratios as a function of rapidity. The vertical lines show the statistical errors while the caps indicate the combined statistical and systematic errors.

the relationship $K^-/K^+ = (\bar{p}/p)^{1/3}$ represents quick calculation based on quark counting and the observation in Ref. 27 that the chemical potentials of baryons μ_B and quarks μ_q have a simple relationship $\mu_B = 3\,\mu_q$ and the μ_s for the chemical potential of strange particles vanishes. The solid line in Fig. 5 represents the statistical model calculation by Becattini [28] *et al.* with parameter inputs from the SPS results assuming T = 170 MeV. With the assumption of local chemical equilibrium the statistical model predicts for $\sqrt{s_{NN}}$ = 200 GeV the baryon chemical potential to be μ_B = 130 MeV at $y \approx 3$ and μ_B = 25 MeV at $y \approx 0$.

V. RAPIDITY DEPENDENT NET-PROTON YIELD

The net-proton yields $[N(p) - N(\bar{p})]$ have been measured at several rapidities in central Au + Au collisions at $\sqrt{s_{NN}}$ = 200 GeV. The data set used for this analysis were collected at a few selected rapidities: $y \approx 0$ and ≈ 0.8 and ≈ 2.9. Figure 6 shows the rapidity densities for $p, \bar{p}$ and p-$\bar{p}$ for 0–10 % central events. This is a dramatic decrease in the net proton yield compared to SPS energy [30], indicating that substantial transparency has been achieved in these collisions. The rapidity dependency of the yield exhibits a boost-invariant behavior of the rapidity plateau for approximately two units of central rapidity.

VI. HIGH p_T MEASUREMENTS

The hadronic charged particle spectra of high p_T are measured from Au + Au collisions at $\sqrt{s_{NN}}$ = 200 GeV
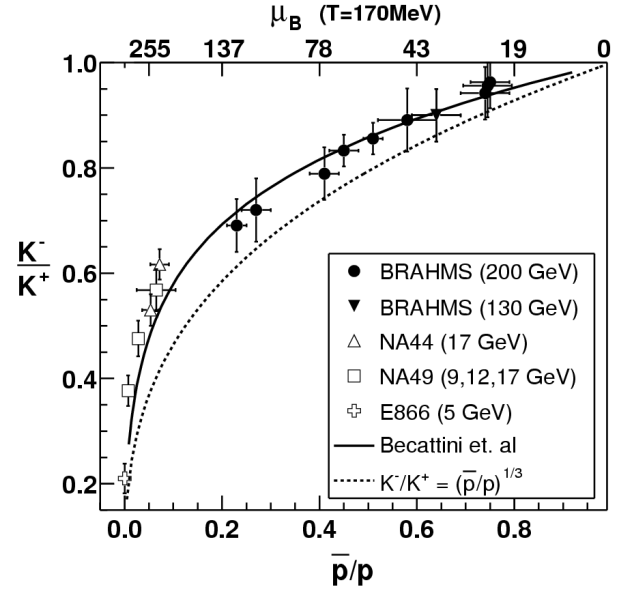

Fig. 5. Correlation between strange meson and baryon antiparticle-to-particle ratios. The NA44 and NA49 data are from Refs. 26 and 25, respectively. The E866 data are from Ref. 24. The dotted line shows $K^-/K^+ = (\bar{p}/p)^{1/3}$. The full line shows the thermal prediction of Becattini *et al.* [28].
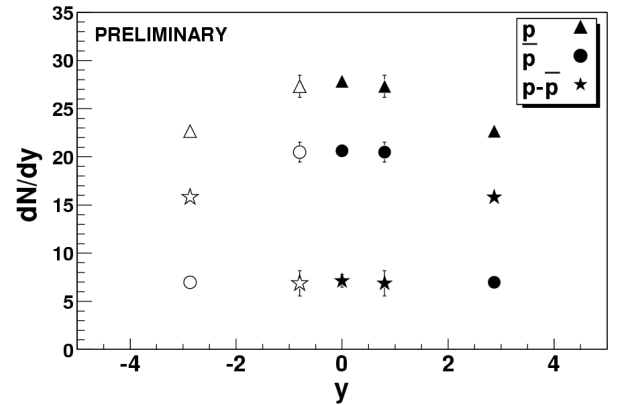

Fig. 6. The Rapidity densities (dN/dy) for p, $\bar{p}$ and p-$\bar{p}$ for central collisions (0–10 %). Closed symbols refer to the measured points and open symbols are values obtained by reflection the measured data about mid-rapidity. the errors are statistical only.

and the data are now under active analysis. The preliminary analysis of the shape of spectra at midrapidity up to 5 GeV indicates a significant medium effect when they are compared to nucleon-nucleon reference spectra [31]. Negative pion spectra have been measured at $y = 2.2$ and the change in spectral shape was observed from central to semi-peripheral collisions.

With detector upgrade in progress the BRAHMS is poised to measure high p_T spectra over a broad range of rapidity, and utilize the upcoming d + Au beams at the RHIC to obtain reliable reference spectra to remove

ambiguities in the interpretation of the medium effect.

VII. CONCLUSIONS

The data for the pseudorapidity density of charged particles are well reproduced by the gluon saturation model of Kharzeev and Levin [3] and also by the pQCD inspired AMPT model [4] based on HIJING [1] microscopic parton model. The present data in the high rapidity regions are consistent with the predictions of the limiting fragmentation model [15]. The antiparticle-to-particle ratios are well reproduced by calculations within the framework of the statistical model with parameter inputs from the SPS [30] experiments or RHIC experiments at $\sqrt{s_{NN}} = 130$ GeV [23,28,29]. The correlations between ratios K^-/K^+ and $\bar{p}/p$ suggest a simple empirical relationship between light and strange quark chemical potentials over a wide range of kinematic variables. The antiparticle-to-particle ratios and the net proton yield measurements at $\sqrt{s_{NN}} = 200$ GeV show significant increase in reaction transparency compared to lower energies.

ACKNOWLEDGMENTS

REFERENCES

[1] X. N. Wang and M. Gyulassy, Phys. Rev. D **44**, 3501 (1991).

[2] K. K. Eskola *et al.*, Phys. Lett. B **497**, 39 (2001).

[3] D. Kharzeev and E. Levin, nucl- th/0108006 and private communication.

[4] Bin Zhang, C. M. Ko, Bao-An Li and Zi-wei Lin, Phys. Rev. C **61**, 067901 (2001).

[5] Zi-wei Lin, Subrata Pal, C. M. Ko, Bao-An Li and Bin Zhang, Phys. Rev. C **64**, 011902R (2001).

[6] Zi-wei Lin, Subrata Pal, C. M. Ko, Bao-An Li and Bin Zhang, Nucl. Phys. A **698**, 375c (2002); nucl-th/0105044; Zi-wei Lin, private communication.

[7] I. G. Bearden *et al.*, Phys. Lett. B **523**, 227 (2001); nucl-ex/0108016.

[8] I. G. Bearden *et al.*, submitted to Nucl. Instrum. Methods A (2002).

[9] I. G. Bearden *et al.*, Phys. Rev. Lett. **88**, 202301 (2002).

[10] B. B. Back *et al.*, Phys. Rev. Lett. **85**, 3100 (2000).

[11] C. Adler *et al.*, Phys. Rev. Lett. **87**, 112303 (2001).

[12] K. Adcox *et al.*, Phys. Rev. Lett. **86**, 3500 (2001).

[13] B. B. Back *et al.*, Phys. Rev. Lett. **88**, 022302 (2002); nucl-exp/0108009.

[14] GEANT 3.2.1, CERN Program Library.

[15] J. Benecke, *et al.*, Phys. Rev. **188**, 2159 (1969).

[16] P. Deines-Jones *et al.*, Phys. Rev. C **62**, 014903 (2000).

[17] G. J. Alner *et al.*, Z. Phys. C **33**, 1 (1986).

[18] I. G. Bearden *et al.*, BRAHMS Collaboration, Phys. Rev. Lett. **87**, 112305 (2001).

[19] I. G. Bearden *et al.*, BRAHMS Collaboration, submitted to Phys. Rev. Lett. (2002).

[20] B. B. Back *et al.*, PHOBOS Collaboration, nucl-ex/0206012.

[21] B. B. Back *et al.*, PHOBOS Collaboration, Phys. Rev. Lett. **87**, 102301 (2001).

[22] C. Adler *et al.*, STAR Collaboration, Phys. Rev. Lett. **86**, 4778 (2001).

[23] P. Braun-Munzinger *et al.*, Phys. Lett. B **518**, 41 (2001).

[24] L. Ahle *et al.*, E866 Collaboration, Phys. Rev. Lett. **81**, 2650 (1998); Phys. Rev. C **60**, 044904 (1999).

[25] Y. Afanasiev *et al.*, NA49 Collaboration, nucl-ex/02050002; J. Bächler *et al.*, Nucl. Phys. A **661**, 45 (1999).

[26] I. G. Bearden *et al.*, NA44 Collaboration, J. Phys. G **23**, 1865 (1997).

[27] P. Koch *et al.*, Phys. Rep. **142**, 167 (1986).

[28] F. Becattini *et al.*, Phys. Rev. C **64**, 024901 (2001) and private communication.

[29] J. Cleymans *et al.*, Z. Phys. C **57**, 135 (1993).

[30] I. Bearden, *et. al.*, NA44 Collaboration, Phys. Rev. C **66**, 044907 (2002).

[31] C. E. Jorgensen, BRAHMS Collaboration, *Proceedings of the Quark Matter 2002* (Nantes, July, 2002) to be published in Nucl. Phys. **A** (2003).